

# A universal velocity distribution of relaxed collisionless structures

Steen H. Hansen<sup>†</sup>, Ben Moore<sup>†</sup>, Marcel Zemp<sup>†‡</sup>, & Joachim Stadel<sup>†</sup>

<sup>†</sup> University of Zurich, Winterthurerstrasse 190, CH-8057 Zurich, Switzerland

<sup>‡</sup> ETH Zurich, Schafmattstrasse 16, Hönggerberg, CH-8093 Zurich, Switzerland

(Dated: December 2, 2024)

The shape of the velocity distribution (VDF) of self-gravitating dark matter structures is in general unknown, and it is also not clear how strongly it depends on initial conditions. We explore the VDF within relaxed collisionless structures that have undergone violent restructuring using high resolution N-body simulations. From hierarchical cold dark matter haloes to monolithic collapse simulations we find that the VDF has a universal shape that can be specified with only one free parameter, the total dispersion. Therefore the final VDF does not depend on the initial conditions as long as the structure has been perturbed sufficiently strongly. The VDF declines much more rapidly than a Gaussian at high energies. We present an analytical fit, which can be used for elliptical galaxy modelling or dark matter detection experiments.

## INTRODUCTION

Various studies have addressed the global properties of equilibrium structures that form via gravitational collapse. The aim was to understand if such evolution can lead to systems that resembled star clusters, elliptical galaxies or galaxy clusters. More recently the emphasis has moved to following the hierarchical growth of structures within a cold dark matter universe (e.g. [1] and references within).

The abundance of dark matter in the universe is very well established [2, 3], however, the nature and properties of the dark matter remains a mystery. One question that needs to be addressed concerns the velocity distribution (VDF) of dark matter. Underground direct detection experiments need the velocity distribution of the dark matter to predict the expected detector signal. Whereas the distribution of classical particles follow a Maxwell-Boltzmann distribution,  $f(v) \sim \exp(-(v/v_0)^2)$ , where  $v_0$  is related to the temperature, we do not know what the shape of this VDF should be for a general self-gravitating dark matter structure. The only thing we know for sure is that it is in general different from a Gaussian (see [4] for references). Cosmological numerical simulations have considered the shape of the VDF [5, 6, 7], and confirmed that the Gaussian shape in general does not give a good fit. Only for the most simple self-gravitating structures, e.g. a Jaffe model or isotropic polytropes, is the actual shape of the VDF known. It is, however, also known that all collisionless structures which have undergone violent processes of restructuring are not isotropic [8], and this means that the radial and tangential VDF's in general will be different.

Structures that form via gravitational collapse and mergers tend to follow universal relationships such that the density profile, radius, anisotropy and phase space density may have strong interdependencies. We will here address the question of the velocity distribution by considering a range of N-body experiments which have undergone significant violent restructuring and subse-

quently have been allowed to relax. We will show that the VDF for all the equilibrated structures has a similar form, one that is well fitted with one free parameter which can be chosen to be the velocity dispersion.

## NUMERICAL SIMULATIONS

The first simulation is a head-on collision between two initially spherical and isotropic NFW structures [9, 10] of  $10^{12}$  solar masses, each with one million particles. For the construction of all the initial structures used in this paper, we use the method described in ref. [4]. The relative velocity between the two haloes is 100 km/sec and the initial separation of the centres is 2000 kpc, which is well outside the virial radius. After several crossings the structure relaxes into a prolate structure. We run all simulations until there is no further time variation in the radial dependence of the anisotropy and density. We check that there is no (local) rotation. All simulations were carried out using PKDGRAV, a multi-stepping, parallel code [11], which uses spline kernel softening and multi-stepping based on the local acceleration of particles. The softening parameter is set to be 0.2% of the virial radii.

In order to extract the velocity distribution we divide the final equilibrated structure into bins in potential. The particles in a given potential bin make up a shape which is well approximated with a triaxial ellipsoid. For each potential bin we calculate the axis-ratios by diagonalization of the shape matrix,  $(\sum x_i^2, \sum x_i y_i, \sum x_i z_i, \dots)$ . We split the velocities for each particle into the part tangential to this ellipsoid and perpendicular to this ellipsoid. In this way we can extract the perpendicular and the tangential VDF. For spherical structures the perpendicular VDF is naturally just the radial VDF. We confirm that using spherical symmetry for the extraction of the radial VDF has little influence on the results, since the potential bins are usually sufficiently close to being spherical.

The resulting structures, from the simulations to be discussed below, have axial ratios that vary as function

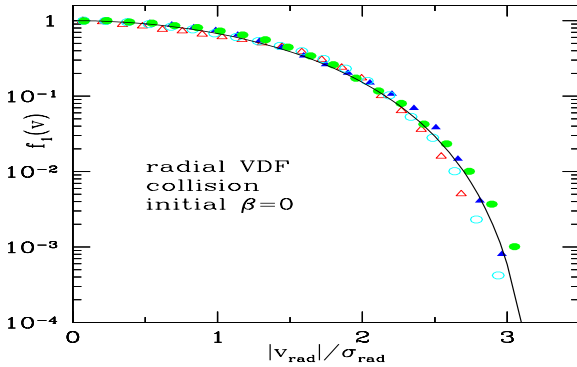


FIG. 1: The radial VDF as function of velocity calculated with respect to iso-potential surfaces. The relaxed equilibrium structure resulted from a radial merger between two initially isotropic NFW haloes. For each potential bin the 1-dimensional radial velocity distribution  $f_1(v)$  is extracted (coloured symbols). The velocities are scaled with the radial dispersion. The solid line is the form of eq. (1), using an entropic index of  $q = 0.8$  and  $\kappa_1 = 1.46$ .

of radius, changing from almost spherical, over prolate or oblate structures, to triaxial structures. Our most conservative constraints on equilibration and mixing is that the *density* bins visually look like triaxial structures (that they don't have significant substructure) and we consider only the central region where this is fulfilled. The density is calculated from the nearest 32 neighbours. It is important to our findings that sufficient equilibration and mixing has occurred. With too little mixing (e.g. at early times) the density bins may not look like any elliptical structure. Concerning resolution in the high density region, we are being rather conservative and exclude a central triaxial region of the equilibrated structure with short axis of 10 times the softening.

We split the final equilibrated region for each simulation into 10 bins in potential (logarithmic separation), and in the figures we plot the VDF's for the 4 bins numbered 2,4,6 and 8. Each potential bin was split into 20 velocity bins, which are presented as coloured symbols. The magnitude is normalized to unity.

In Figure 1 we present the radial VDF of the first simulation, where the velocities are scaled with the radial dispersion. As is clear from this figure, the VDF's in these 4 bins have approximately the same shape when scaled with the radial dispersion. In all figures we use green (filled) circles for the inner-most bins, and red (open) triangles for the outer-most bins. We also plot a fit-by-eye of the shape

$$f(v) = \left( 1 - (1 - q) \left( \frac{v}{\kappa_1 \sigma_{\text{rad}}} \right)^2 \right)^{\frac{q}{1-q}}, \quad (1)$$

where  $q$  and  $\kappa_1$  are free parameters. We use  $q = 0.8$  and

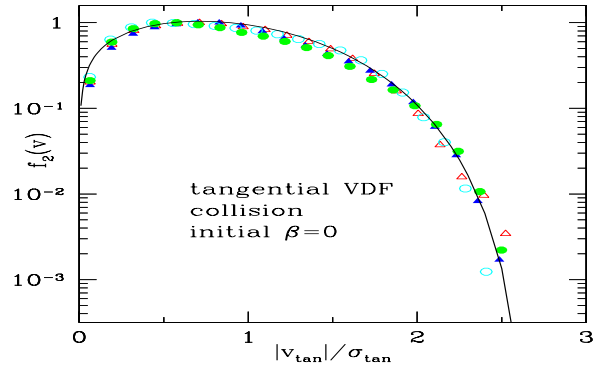


FIG. 2: The 2-dimensional tangential VDF  $f_2(v)$  for the same simulation as in Figure 1. The velocities are scaled with the tangential dispersion. The solid line is the form of eq. (2), using entropic index of  $q = 0.8$  and  $\kappa_2 = 1.21$ .

$\kappa_1 = 1.46$ . This is the Tsallis form [12], and depends on the entropic index  $q$ . This form reduces to the Gaussian shape  $f(v) \sim \exp(-(v/v_0)^2)$  when  $q = 1$ . This functional form is chosen partly for simplicity (and because it includes the classical exponential), and partly because some simple structures are known to have VDF's of exactly this form [13, 14]. It is interesting to note that ref. [7] found that the radial VDF of the inner-most bin is fit with a Gaussian  $q = 1$ , and the intermediate bins can be fitted with  $q = 0.65$ .

In Figure 2 we present the tangential VDF, where the velocities are scaled with the tangential dispersion. As is clear from this figure, the VDF's in these 4 bins have approximately the same shape when scaled with the tangential dispersion. We also plot a fit-by-eye of the shape

$$f(v) = v^{2q-1} \left( 1 - (1 - q) \left( \frac{v}{\kappa_2 \sigma_{\text{tan}}} \right)^2 \right)^{\frac{q}{1-q}}, \quad (2)$$

where again  $q$  and  $\kappa_2$  are free parameters. We use  $q = 0.8$  and  $\kappa_2 = 1.21$ . Again, this form reduces to the Gaussian shape  $f(v) \sim v \exp(-(v/v_0)^2)$  when  $q = 1$ . The exponent of the velocity,  $2q - 1$ , is chosen almost randomly. One could argue that  $3q - 2$  is more natural (in 3 dimensions), however, this provides a slightly worse fit.

In Figure 3 we present the full 3-dimensional VDF, where velocities have been scaled with the total dispersion,  $\sigma_{\text{tot}}^2 = \sigma_{\text{rad}}^2 + \sigma_{\text{tan}}^2$ . The anisotropies of the different bins are different. The full line is a fit of the form

$$f(v) = v^{2q} \left( 1 - (1 - q) \left( \frac{v}{\kappa_3 \sigma_{\text{tot}}} \right)^2 \right)^{\frac{q}{1-q}}, \quad (3)$$

where we used  $q = 0.8$  and  $\kappa_3 = 0.95$ . Using the more natural  $3q - 1$  instead of  $2q$  in the exponent of the velocity leads to an equally good fit with virtually unchanged  $q$

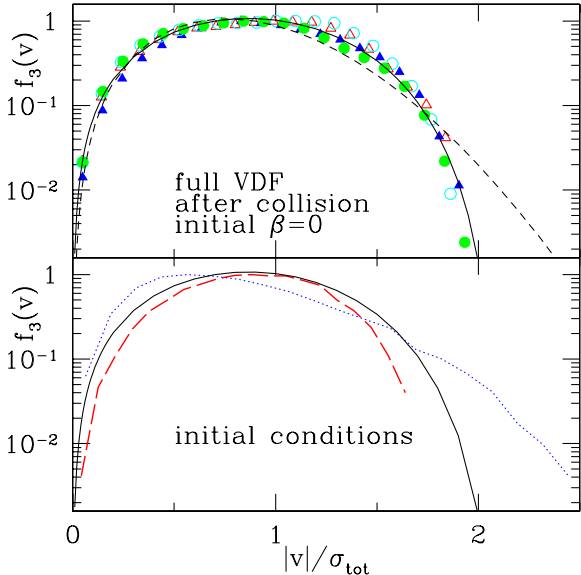


FIG. 3: The full 3-d VDF  $f_3(v)$  for the same simulation as in Figure 1. The velocities are scaled with the total dispersion. The solid line is the form of eq. (3), using entropic index of  $q = 0.8$  and  $\kappa_3 = 0.95$ . The dashed line is a Gaussian. The lower panel are two bins from the initial condition which visibly are different from each other. The black line is the same as in the upper panel.

and  $\kappa_3$ . The dashed line is a Gaussian with  $q = 1$ , which provides a bad fit in the high-velocity part. The fits are visibly worse if using values of  $q$  or  $\kappa$  which are 10% different. The lower panel in Fig. 3 shows two bins from the initial conditions (red long-dashed is from the outer region, blue dotted from the inner region). The fact that the initial VDF are different in different regions is well-known [15].

In order to test the stability of these resulting VDF's, we will now study even more perturbed systems. We take two copies of the resulting structure (each with 2 million particles), and collide these two (again initially well separated structures) with relative velocity of 100 km/sec. The final equilibrated region contains approximately 3 million particles. The result is shown in the top panel of Figure 4. The solid line is the *same* as plotted in Figure 3 to show the similarity.

To address the question of how strongly the VDF's from the head-on collisions described above depend on the initial conditions, we now consider 2 simulations each with two steps. i) First we create a spherical isotropic NFW structure with 1 million particles. We take each particle and put its total velocity along the radial direction, maintaining the sign with respect to inwards or outwards from the halo centre. We keep the energy of each particle fixed. This structure is thus strongly ra-

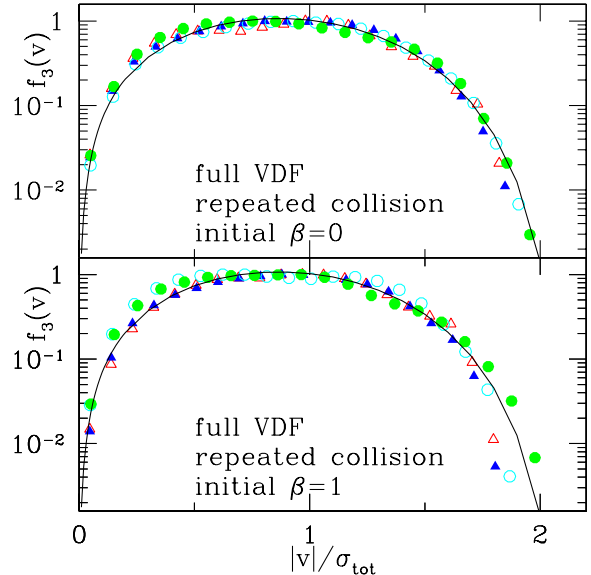


FIG. 4: Same as Figure 3, but for a *repeated* head-on collision of 2 initially isotropic NFW structures (coloured symbols, top panel). The lower panel is for radially anisotropic initial conditions. The solid lines are the *same* line as in Figure 3, using the same values for  $q$  and  $\kappa_3$ .

dially anisotropic. ii) Now we take two such radially anisotropic structures and place their centres 2000 kpc apart (well outside the virial radius) with relative velocity of 100 km/sec towards each other. Before the centres of the two structures collide the radial motion of the particles behaves almost like a radial infall simulation, and strong scattering of the particles is observed. The 2 individual structures pick random orientations in space as they become triaxial [16]; their orientations are completely erased after the two structures collide head-on. We take the resulting structures and collide them head-on, again with 100 km/sec. The final equilibrated region contains approximately 2.5 million particles. The result of this simulation is shown in the lower panel of Fig. 4. The solid line is again the exact same as the one shown in Figure 3. The scatter is slightly larger than previously, and when looked at the density plot of the simulation it is clear that this simulation is still not completely mixed. The radial and tangential VDF's (not shown here) also have a universal shape, which is given by eqs. (1, 2), with the same parameters,  $q, \kappa_1$  and  $\kappa_2$ . We run a simulation identical to the one just described, except that we place all the particles in the initial structures on tangential orbits, without changing the energy of the individual particles. The VDF resulting after the collisions (not presented here) again follows the same curve with the same  $q$  and  $\kappa_3$ . We also run a spherical collapse of an initial  $r^{-1}$  density profile with 1 million particles, and the resulting

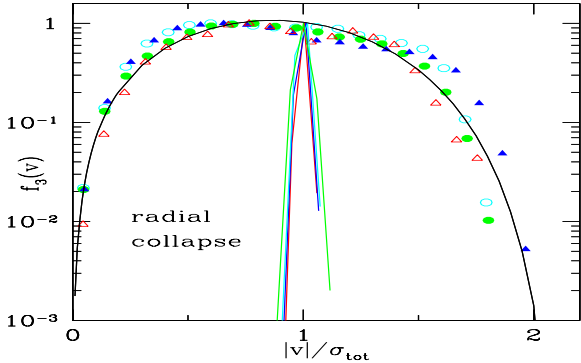


FIG. 5: The full VDF of a radial collapse simulation. The solid line is the *same* line as in Figure 3, using the same values for  $q$  and  $\kappa_3$ . The lines near  $v = \sigma$  are the VDF from a very early stage of the simulation, where all the particles are moving almost radially.

VDF, shown in Figure 5, again follows roughly the same curve with the same  $q$  and  $\kappa_3$ , however, it looks slightly more flat-topped.

Finally we consider simulated cosmological  $\Lambda$ CDM haloes that form in a standard expanding hierarchical universe. We analyse these haloes in the same way as above, and we observe that the haloes in the process of undergoing a merger are slightly distorted from the universal shape described above. The more active ongoing mergers have more flat-topped VDF for  $v > \sigma_{\text{tot}}$ , but a similar fall-off near  $v \sim 2\sigma_{\text{tot}}$ . Perhaps these more flat-topped VDF's reflect structures which are still not fully mixed. The substructure has a marginal effect on the VDF's in the centrally equilibrated region. We present two relaxed halos in Figures 6 and 7, each with approximately 1/2 million particles in the equilibrated region. These are the two binary haloes taken from the Local Group simulation of [5]. One of these haloes is strongly oblate, the other strongly prolate. The solid lines are identical to those used numerous time above. We therefore see that there is a striking concordance between the various numerical experiments.

## CONCLUSIONS

We consider the velocity distribution (VDF) from a large range of numerical simulations, where the initial configurations include isotropic and highly non-isotropic structures, as well as cosmological CDM structures. These structures have in common that they have been perturbed violently and subsequently allowed to relax. These resulting structures include almost spherical and highly triaxial structures, and we extract the VDF in potential bins of these ellipsoids. We show that the VDF

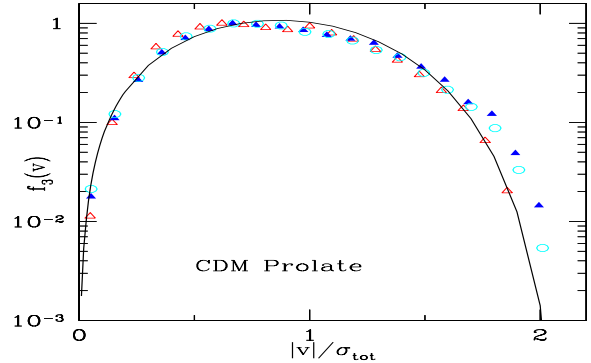


FIG. 6: A cosmological CDM simulations of a prolate structure. The solid line is the *same* line as in Figure 3, using the same values for  $q$  and  $\kappa_3$ .

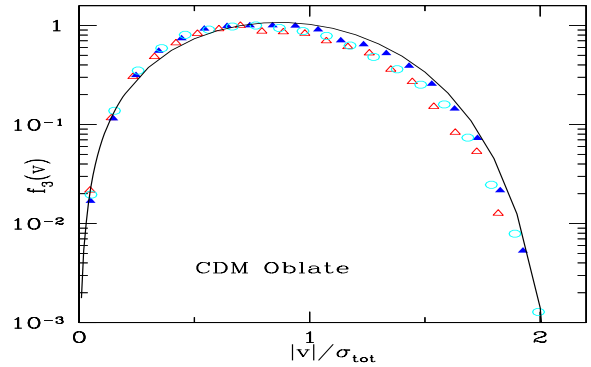


FIG. 7: A cosmological CDM simulations of an oblate structure. The solid line is the *same* line as in Figure 3, using the same values for  $q$  and  $\kappa_3$ .

has a universal shape. We present a fit to this shape, which depends only on one free parameter, the total velocity dispersion. The fit is given in eq. (3).

This VDF should be convolved with the detector response for dark matter experiments, in order to analyse correctly the events. The shape has a cut-off at high momentum, and hence the normal Gaussian tail is absent.

This numerical discovery is an important step towards a fundamental understanding of the behaviour of structures that form via violent relaxation, such as dark matter haloes, and a theoretical understanding hereof would be highly interesting.

## Acknowledgments

It is a pleasure to thank Victor Debattista and David Merritt for interesting suggestions, and Ewa Lokas and

Gary Mamon for useful comments. SHH thanks the Tomalla foundation for financial support.

---

[1] S. Ghigna, B. Moore, F. Governato, G. Lake, T. Quinn and J. Stadel, *Astrophys. J.* **544** (2000) 616 [arXiv:astro-ph/9910166].

[2] D. N. Spergel *et al.* [WMAP Collaboration], *Astrophys. J. Suppl.* **148** (2003) 175 [arXiv:astro-ph/0302209].

[3] M. Tegmark *et al.* [SDSS Collaboration], *Phys. Rev. D* **69** (2004) 103501 [arXiv:astro-ph/0310723].

[4] S. Kazantzidis, J. Magorrian and B. Moore, *Astrophys. J.* **601** (2004) 37 [arXiv:astro-ph/0309517].

[5] B. Moore, C. Calcareo-Roldan, J. Stadel, T. Quinn, G. Lake, S. Ghigna and F. Governato, *Phys. Rev. D* **64** (2001) 063508

[6] J. Diemand, B. Moore and J. Stadel, *Mon. Not. Roy. Astron. Soc.* **352** (2004) 535 [arXiv:astro-ph/0402160].

[7] R. Wojtak, E. L. Lokas, S. Gottloeber and G. A. Mamon, *MNRAS* (in press), arXiv:astro-ph/0503391.

[8] S. H. Hansen and B. Moore, arXiv:astro-ph/0411473.

[9] J. F. Navarro, C. S. Frenk and S. D. M. White, 1996, *ApJ*, 462, 563

[10] S. H. Hansen, *Mon. Not. Roy. Astron. Soc.* **352** (2004) L41 [arXiv:astro-ph/0405371].

[11] Stadel J., 2001, PhD thesis, University of Washington

[12] C. Tsallis, *J. Stat. Phys.* **52**, 479 (1988)

[13] Plastino, A. R. & Plastino, A. 1993, *PLA*, 173, 384

[14] S. H. Hansen, D. Egli, L. Hollenstein and C. Salzmann, *New Astron.* **10** (2005) 379 [arXiv:astro-ph/0407111].

[15] D. Merritt, *ApJ* **313** (1987) 121

[16] D. Merritt, *MNRAS* **217** (1985) 787